Desalination and Water Treatment
www.deswater.com
doi: 10.5004/dwt.2019.24514

166 (2019) 387–398
October

Removal of basic and acid dyes from aqueous solutions using cone powder from Moroccan cypress *Cupressus sempervirens* as a natural adsorbent

Zineb Bencheqroun[a], Imane El Mrabet[a], Mohammed Kachabi[a], Mostafa Nawdali[b], Héctor Valdés[c], Isabel Neves[d,e], Hicham Zaitan[a,*]

[a]*Chemistry of Condenser Matter Laboratory (LCMC), Faculty of Science and Technology, Sidi Mohamed Ben Abdellah University, B.P. 2202, Fez, Morocco, emails: hicham.zaitan@usmba.ac.ma (H. Zaitan), zinebbencheqroun@yahoo.fr (Z. Bencheqroun), imane.elmrabet@usmba.ac.ma (I. El Mrabet), mohammed.kachabi@usmba.ac.ma (M. Kachabi)*
[b]*Laboratory LCMC, Faculty of Polydisciplinary, Sidi Mohamed Ben Abdellah University, B.P 1223, Taza, Morocco, email: mostafa.nawdali@usmba.ac.ma*
[c]*Clean Technologies Laboratory, Universidad Católica de la Santísima Concepción, Alonso de Ribera 2850, Concepción, Chile, email: hvaldes@ucsc.cl*
[d]*CQUM, Center of Chemistry, Chemistry Department, University of Minho, 4710-057 Braga, Portugal, email: ineves@quimica.uminho.pt*
[e]*CEB – Center of Biological Engineering, University of Minho, 4710-057 Braga, Portugal*

Received 10 December 2018; Accepted 9 June 2019

ABSTRACT

This study aims to evaluate the technical feasibility of applying a low-cost alternative natural bioadsorbent obtained from the cone of the Moroccan cypress *Cupressus sempervirens* to remove dyes from contaminated waters. Methylene Blue (MB) and Congo Red (CR) dyes are used to represent basic and acid compounds present in wastewater of textile industries. The cone of this medium-sized coniferous evergreen tree was obtained from the Fez area and was characterised by different physical–chemical methods, including nitrogen adsorption–desorption isotherms, Fourier transform infrared spectroscopy, scanning electron microscopy, Boehm titration method and the pH of the point of zero charge (pH_{pzc}). Additionally, the influence of operating conditions such as contact time, initial dye concentration, binary mixture of dye solutions, bioadsorbent dosages and solution pH were evaluated. Experimental results reveal that the adsorption processes take place very rapidly, reaching equilibrium at 30 and 45 min for MB and CR, respectively. Maximum adsorption capacities result to be pH dependents. Hence, MB adsorption is favoured under basic pH conditions, while CR is favoured at acidic pH. A pseudo-second-order kinetic model provides the best fit of the experimental data of MB and CR adsorption onto the biomaterial. Adsorption isotherm data are well represented by Langmuir, Freundlich and Dubinin–Radushkevich models. Langmuir model gives the best fit with a maximum monolayer sorption capacity of 144 and 25.02 mg g^{-1} for MB and CR, respectively. Experimental results indicate that the cone of *Cupressus sempervirens* could be used as a potential, low-cost bioadsorbent for the elimination of dyes from contaminated waters.

Keywords: Adsorption; Low-cost natural bioadsorbent; Textile dyes

1. Introduction

Currently, a great variety of dyes are used in papermaking, textile, food and pharmaceutical industries [1]. The presence of synthetic dyes in ecosystems poses a serious environmental and health threats, because most of them are toxic, mutagenic and carcinogenic [2].

These pollutants must be removed from wastewater streams to acceptable levels by appropriate methods. Because

* Corresponding author.

of its low cost and operational simplicity, adsorption is widely used for the removal of dye pollutants from aqueous solutions [3,4]. Activated carbon is a good adsorbent for wastewater treatment applications; however, it is very expensive and it should be discharged after use. Therefore, the development of effective and low-cost alternative adsorbents for the removal of dyes is attracting more and more attention from worldwide researchers [5].

In this context, natural adsorbents appear as interesting alternatives for cleaning polluted waters, since their application could result in a cost-effective process for dye removal. In this study, the technical feasibility of using inexpensive materials such as cones of *Cupressus sempervirens* as agricultural wastes is studied as a cheap alternative to expensive commercial activated carbons for removing colorants from waters. Among natural adsorbents, cones of *Cupressus sempervirens* (CCS) are found abundantly as agricultural waste in Morocco. Hence, they are likely to become strong candidates as a bioadsorbent in the removal of dyes from aqueous solutions.

In this study, batch experiments using a Moroccan CCS from the Fez area as a bioadsorbent were carried out to determine the effect of different adsorption parameters such as pH, initial dye concentration, contact time and adsorbent dosages. Adsorption kinetics of Methylene Blue (MB) and Congo red (CR) dyes were evaluated by pseudo-first-order and pseudo-second-order kinetic models. Adsorption equilibrium was modelled using Langmuir, Freundlich and Dubinin–Radushkevich equations. The surface properties of the bioadsorbent were characterised by several techniques, such as N_2 adsorption isotherms, scanning electron microscopy (SEM) analyses and acid-base neutralisation method. Adsorption studies were performed using single dye molecules and binary mixtures. Additionally, MB and CR interactions with active sites of CCS surface were identified by Fourier transform infrared spectroscopy (FTIR) analysis.

2. Materials and methods

2.1. Materials

Samples of CCS were collected from the Fez area in Morocco, washed with tap water several times and then with distilled water in order to eliminate impurities present on the surface. Samples were dried in an oven at 110°C for 24 h, cut into small portions, and crushed using a domestic grinder. After that, grinded samples were sieved and particle sizes (<100 μm) were used in all experiments. Samples were stored in hermetic glass bottles. Fig. 1 shows the raw material and the grinded forms of the prepared bioadsorbent.

Two different commercial dyes were employed in this study: Methylene Blue (MB; $C_{16}H_{18}ClN_3S$; Mw = 319.85 g mol^{-1}; λ_{max} = 664 nm) and Congo red (CR, $C_{32}H_{22}N_6Na_2O_6S_2$, Mw = 696.66 g mol^{-1}, λ_{max} = 500 nm). They were provided by Sigma-Aldrich Chimie S.a.r.l. (Lyon, France) and were used without any further purification.

2.2. Characterisation of the natural bioadsorbent

Specific surface area and pore volume of the CCS were determined from N_2 adsorption–desorption isotherms at –196°C using a Micromeritics ASAP 2010 sorptometer (Micromeritics Corporate Headquarters, Norcross, GA, USA). Sample of CCS was degassed before analysis at 110°C for 10 h under vacuum at $<10^{-2}$ Pa, in order to remove all physically adsorbed water molecules and small organic impurities. Chemical surface composition of the CCS before and after adsorption of MB and CR was identified by FTIR, using a VERTEX70 spectrometer (Bruker Optics S.a.r.l., France) within the range of 4,000–400 cm^{-1}. Morphological features of CCS were analysed by SEM (FEIPhilips XL30 ESEM, Corporate Headquarters, USA).

The basicity and acidity of the CCS material were estimated using the Boehm titration method [6]. A mass of 1.5 g CCS sample was placed in contact with 40 mL of the following solutions: NaOH (0.1 M), $NaHCO_3$ (0.05 M), Na_2CO_3 (0.05 M) and HCl (0.1 M). After that, the vials were sealed and stirred for 72 h at room temperature and then filtered. A volume of 10 mL of the filtrate was pipetted and the excess of base or acid was titrated with HCl (0.05 M) or NaOH (0.05 M), respectively. The total concentration of acidic sites was determined under the assumption that NaOH neutralises acidic sites of different strength (carboxylic, lactonic and phenolic groups), Na_2CO_3 neutralises carboxylic and lactonic groups on CCS surface, and $NaHCO_3$ neutralises only carboxylic groups. The concentration of basic

Fig. 1. Raw and grinded (60–120 μm particle size) forms of low-cost bioadsorbent CCS.

sites was calculated from the amount of HCl consumed by the CCS.

The pH value required to give a zero net surface charge (pH_{pzc}) was determined through the procedure described by Stumm and Morgan [7]. Briefly, volumes of 50 mL NaCl solutions (0.1 M) were transferred into series of flasks and their initial pH ($pH_{initial}$) was adjusted by adding NaOH or HCl solution between 2 and 12. Then, 0.1 g of CCS was loaded into each flask and Nitrogen was bubbled through the solutions. After that, the flasks were then shaken during 72 h at 25°C. Subsequently, the solution pH of each flask was measured. Finally, the pH_{pzc} was determined graphically where $pH_{final} = pH_{initial}$.

2.3. Adsorption experiments

2.3.1. Singles adsorption studies

Dye adsorption experiments were conducted using a batch method. For that, 10 mg of the CCS was added 20 mL of dye solution with the desired initial dye concentrations (10 to 1,000 mg L^{-1}) without adjustment of pH (pH 7). The mixtures were shaken at 200 rpm until the equilibrium was reached, using a water shaker bath with temperature fixed at 25°C. After that, the solid phases were separated from each solution by centrifugation. Finally, the remaining concentrations of MB and CR were determined by UV/Visible spectrophotometry (UV1600 spectrophotometer). Absorbance values of the solutions were measured at the maximum wavelengths for MB and CR (664 and 500 nm, respectively), as shown in Fig. 2.

The total amount of adsorbed dye per unit mass of CCS at the equilibrium (q_e, mg g^{-1}) and the amount of dye adsorbed at specific time (q_t, mg g^{-1}) were calculated using the following equation:

$$q_{t,e} = \frac{\left(C_0 - C_{t,e}\right)V}{m} \tag{1}$$

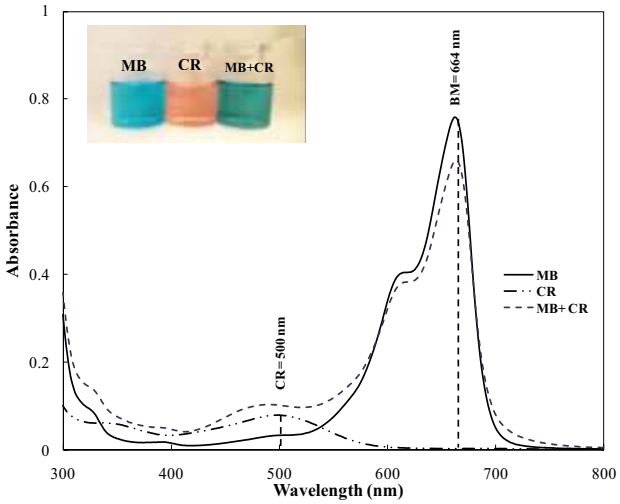

Fig. 2. Typical UV–Vis spectrum of each single solution of MB, CR and a binary solution of both dyes (BM–CR). The inset shows the original colours of the dyes and the mixture.

where C_0 (mg L^{-1}) and $C_{t,e}$ (mg L^{-1}) are the initial and time t or the equilibrium concentrations of dye respectively; m (g) is the mass of bioadsorbent used and V (L) is the volume of the dye solution used in the experiment.

The percentage of dye removal (R, %) was expressed as:

$$R(\%) = \frac{\left(C_0 - C_e\right)}{C_0} \times 100 \tag{2}$$

The effect of operating conditions on dye adsorption was studied. The initial dye concentration was varied between 10 and 1,000 mg L^{-1}. The pH of the solutions was fixed in the range of 2 to 12; whereas the contact time, particle size, bioadsorbent dosages and temperature were adjusted in the range of 0–150 min, 100–500 μm, 0.1–1.0 g and 25°C–45°C, respectively. All tests were performed in triplicates.

2.3.2. Binary adsorption studies

The binary adsorption of Methylene Blue and Congo Red (BM + CR) was assessed in a batch system. The adsorption of the mixture of dyes was carried by adding 0.4 g of CCS into flasks, containing 20 mL of BM + CR solution with a concentration that was varied between 100 and 1,000 mg L^{-1} at 25°C. Experiments were carried out following the same steps as previously described for a single dye adsorption process. The concentration of MB and CR in the mixture was determined by measuring the absorbance at λ_{max} MB = 664 nm and λ_{max} CR = 500 nm. Thus, in a binary mixture of components, the concentrations of MB (C_{MB}) and CR (C_{CR}) were calculated as follows [8,9]:

$$C_{MB} = \frac{k_{CR_2} d_1 - k_{CR_1} d_2}{k_{MB_1} k_{CR_2} - k_{MB_2} k_{CR_1}} \tag{3}$$

$$C_{CR} = \frac{k_{MB_1} d_2 - k_{MB_2} d_1}{k_{MB_1} k_{CR_2} - k_{MB_2} k_{CR_1}} \tag{4}$$

where k_{MB_1}, k_{CR_1}, k_{MB_2} and k_{CR_2} are the calibration constants; whereas d_1 and d_2 represent optical densities for MB and CR at wavelengths λ_1 and λ_2, respectively.

3. Results and discussion

3.1. Characterisation of the bioadsorbent

Fig. 3 displays equilibrium data of the adsorption–desorption of N_2 onto CCS measured at –196°C. CCS exhibits a Type II isotherm with a hysteresis loop, according to the IUPAC classification. Table 1 summarises physico-chemical characteristics of CCS. Results indicate that CCS is predominantly a mesoporous material, with a specific surface area of 27.2 $m^2 g^{-1}$. According to Boehm titration results, the amount of acidic groups is significantly higher than the amount of basic groups. The material shows a pH_{pzc} of 6.0. At pH conditions higher than the pH_{pzc}, the CCS surface will be negatively charged; whereas in the pH region below to the pH_{pzc}, positively charged sites will dominate on the adsorbent surface.

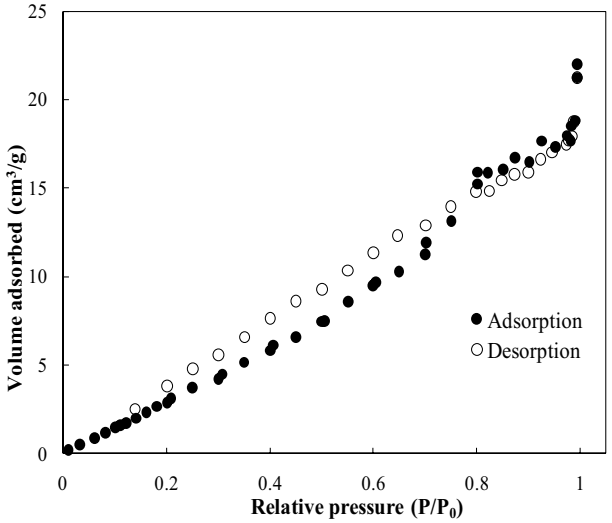

Fig. 3. N_2 adsorption and desorption isotherms of CCS at –196°C.

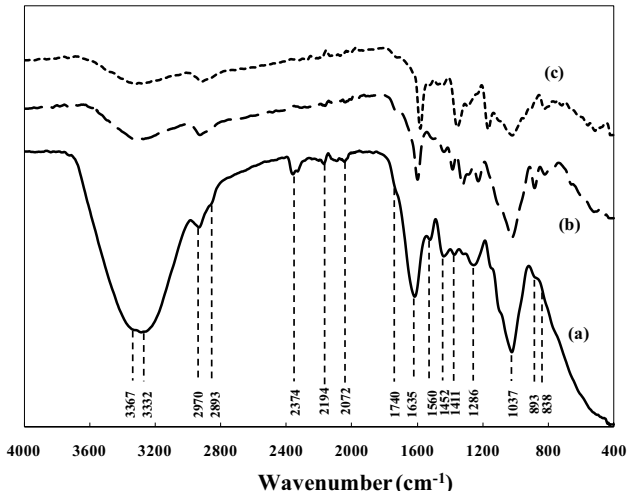

Fig. 4. FTIR spectra of raw adsorbent and adsorbent after adsorption of dye molecules: (a) raw surface of CCS, (b) CCS loaded with MB molecules and (c) CCS loaded with CR molecules.

Table 1
Physico-chemical properties of CCS

Textural properties	
d_p (nm)	3.5
d (cm^3 g^{-1})	0.028
S_{BET} (m^2 g^{-1})	27.2
V_T (cm^3 g^{-1})	0.028
Chemical properties	
pH_{pzc}	6.0
CG (meq L^{-1})	0.1
LG (meq L^{-1})	1.03
PG (meq L^{-1})	0.39
TAS (meq L^{-1})	1.52
TBS (meq L^{-1})	0.87

d_p, mean pore width; d, density, S_{BET}, BET surface area, V_T, total pore volume, pH_{pzc}, pH of zero net surface charge, CG, carboxylic groups, LG, lactonic groups, PG, phenolic groups, TAS, total acid sites, TBS, total basic sites.

Fig. 4 depicts infrared vibrations of functional surface groups of raw CCS and upon the adsorption of dye molecules identified by FTIR analyses. In the FTIR spectra, broad and superimposed bands between 3,200 and 3,500 cm^{-1} are attributed to the typical stretching vibrations of O–H groups [10,11]. The bands at 2,970 and 2,893 cm^{-1} are referred to the C–H stretching vibrations, suggesting the presence of alkane/alkene groups on the CCS surface [12]. The band at 1,740 cm^{-1} is ascribed to C=O stretching vibration of ketones or aldehydes, lactones, or carboxyl groups present in hemicelluloses and lignin. The bands in the region between 2,000 and 2,200 cm^{-1} are attributed to scissoring and rocking vibrations of water. The band at 2,374 cm^{-1} is assigned to the C–O stretching vibrations. The band at 1,635 cm^{-1} in raw material (Fig. 4a) corresponds to bending vibration of O–H groups and is shifted to 1,606 and 1,590 cm^{-1} after MB and CR are loaded onto CCS surface, respectively. It could be due to the involvement of hydrogen from the O–H group in the formation of surface complex with intramolecular hydrogen bonding, which facilitates the sorption of dye molecules onto the adsorbent surface. The bands between 1,000 and 1,500 cm^{-1} on the CCS spectrum (Fig. 4a) are due to the C–OH stretching and –OH bending vibrations, indicating the existence of large numbers of hydroxyl groups (–OH) and carboxylic groups (–COOH) [13]. The presence of carboxylic acid groups in CCS is caused by the presence of cellulose or lignin. The band at 1,452 cm^{-1} confirm the presence of C=C bonds of alkene and aromatic rings. The bands at 1,286 and 1,411 cm^{-1} are attributed to the C–O vibration. A strong band at 1,037 cm^{-1} could be attributed to =C–O–C stretching vibrations. The bands at 893 and 838 cm^{-1} could be due to out-of-plane deformation mode of N-containing bioligands [14]. Functional surface groups such as O–H, C=O and C–O could be potential active sites for the adsorption of MB and CR molecules. Upon the adsorption of dye molecules (Figs. 4b and c), chemical interactions among active sites of CCS surface and dye molecules (MB and CR) are registered. A decrease in the intensity and a shift of O–H (1,635 cm^{-1}) and C–O (1,037 cm^{-1}) bands are observed, indicating an interaction between dyes (MB and CR) and these groups of CCS surface.

SEM images of CCS are shown in Fig. 5. The irregular forms and different sizes of the CCS particles can also be observed. A well-developed surface morphology is clearly visible with the existence of a heterogeneous porous structure.

3.2. Effect of the operating conditions on the adsorption capacity of CCS

Fig. 6 shows the effect of varying the dosage of CCS on MB and CR adsorption in the range from 0 to 1 g L^{-1} with a total volume of solution 20 mL and using a dye concentration of 500 mg L^{-1} at 25°C.

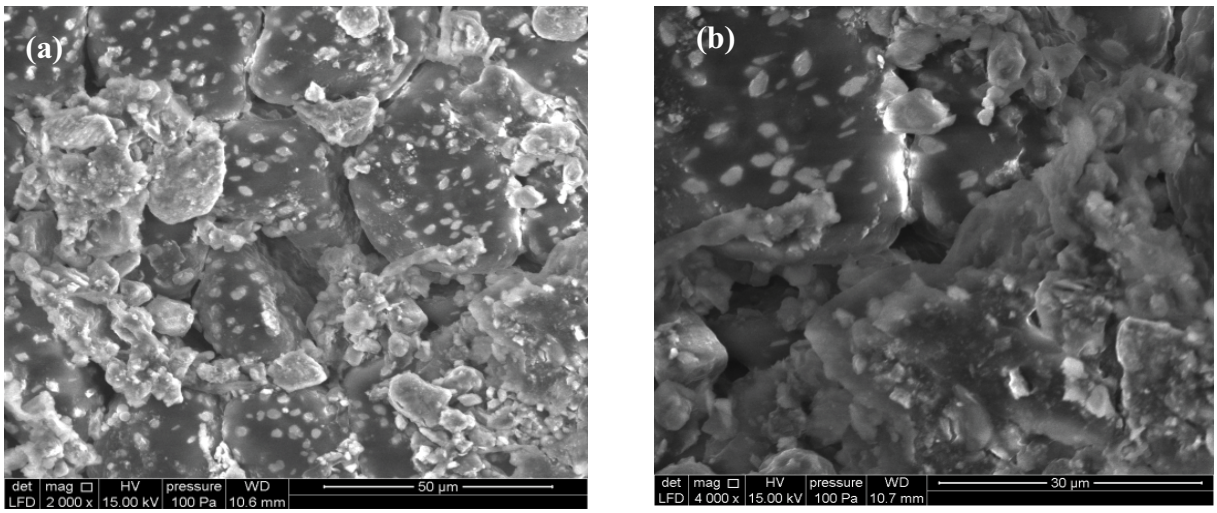

Fig. 5. SEM images of CCS particles (a) (×2,000) and (b) (×4,000).

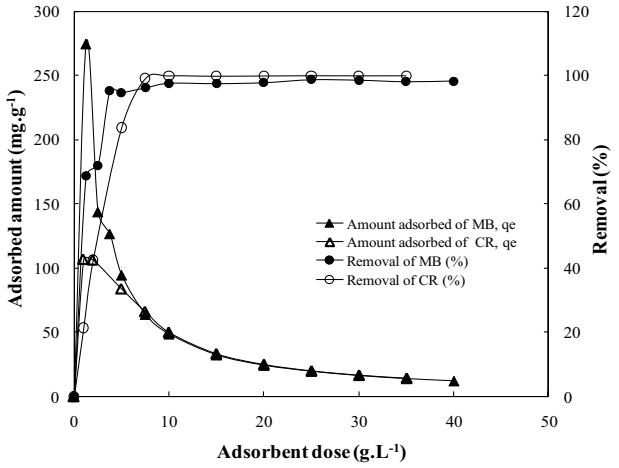

Fig. 6. Effect of the dosages of CCS (0–1 g L^{-1}) on the adsorption capacity towards MB and CR. Operating conditions: C_0 = 500 mg L^{-1}, contact time = 24 h, agitation speed = 200 rpm and T = 25°C.

It is clear that the removal efficiency of MB and CR dyes is increased with the addition of more adsorbent dosages. On one hand, the efficiency of MB is increased from 44% to 98% when CCS amount is raised from 0.025 to 0.100 g L^{-1}. On the other hand, the efficiency of CR is increased from 1% to 84% when the CCS is increased from 0.1 to 0.6 g L^{-1}.

Such results can be attributed to a higher availability of actives sites with the increase in the amount of the bioadsorbent. However, further mass increase of the bioadsorbent dosages does not change removal efficiency, because all MB and CR molecules have already been removed from the solution.

It can also be observed that for an initial concentration of 500 mg L^{-1} of MB, the adsorption capacity of CCS towards MB decreases with the increase of the adsorbent dose, may be due to particle interaction (aggregation). Similar behaviour for the effect of adsorbent concentrations on MB adsorption capacity was observed and discussed in the literature for other types of adsorbents [15,16]. Results indicate that the optimal bioadsorbent concentration for MB and CR dyes is 7.5 and 20 g L^{-1}, respectively.

The effect of pH over a pH range of 2–12 on the adsorption of MB and CR dyes onto CCS is depicted in Fig. 7.

As shown in Fig. 7, the adsorbed amounts are found to be almost constant between pH of 2 and 8 for both dyes with the maximum adsorbed amounts of MB (100 mg g^{-1} equivalent to a removal efficiency of ~99%) and CR (20 mg g^{-1}, equivalent to a removal efficiency of ~79%). Results reveal high levels of pH tolerance of CCS for MB and CR adsorption, which is extremely attractive for practical applications. As the solution became more basic (pH > 8), the adsorption capacity remains constant for MB and the dye removal was not affected, whereas in the case of CR a slight decrease is observed. At pH > 8 > pH_{pzc}, the CCS surface will be negatively charged causing a decrease of the CR adsorbed onto CCS. This result may be due to electrostatic repulsion

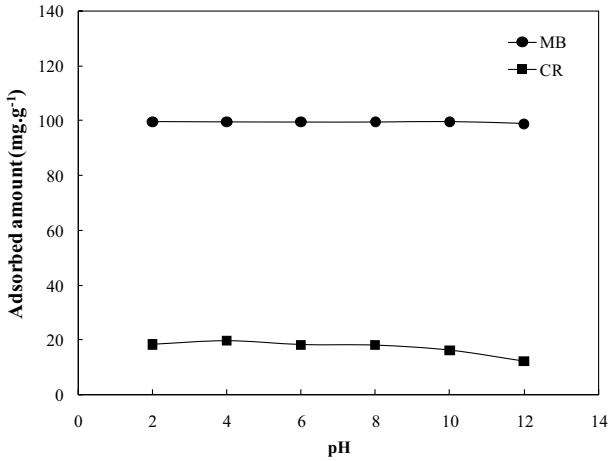

Fig. 7. Effect of pH on the adsorption capacity of CCS towards MB and CR. Operating conditions: C_0 = 500 mg L^{-1}, contact time = 24 h, dose of CCS = 7.5 g L^{-1} (MB) and 20 g L^{-1} (CR), agitation speed = 200 rpm and T = 25°C.

between the negatively charged adsorbent surface and the CR anions. The particle size is an important parameter in the adsorption process. To illustrate the effect of particle size on MB and CR adsorption, four different ranges of CCS particle sizes (<100 μm, 100–200 μm, 200–500 μm, >500 μm) were loaded into flasks containing a volume of 200 mL with a fixed initial concentration (500 mg L^{-1}) of dye solution, at room temperature. Experimental results in terms of the adsorbed amount of dye as a function of contact time are shown in Fig. 8. It can be observed that at equilibrium, the adsorption capacity of CCS decreases from 65.85 to 26.45 mg g^{-1} for MB dye and from 12.7 to 1.69 mg g^{-1} for CR dye, when the particle size is increased from <100 to >500 μm. The high amount of adsorbed dye for smaller particles could be attributed to the fact that smaller particles provide a higher number of available sites for the adsorption of dyes. In addition, the variation of the particle size affects the time required to reach the equilibrium. The observed time to attain the equilibrium increases from 20 to 45 min, as particle size increases from <100 to >500 μm. It is clear that the increase in particle size limits the internal mass transfer rate.

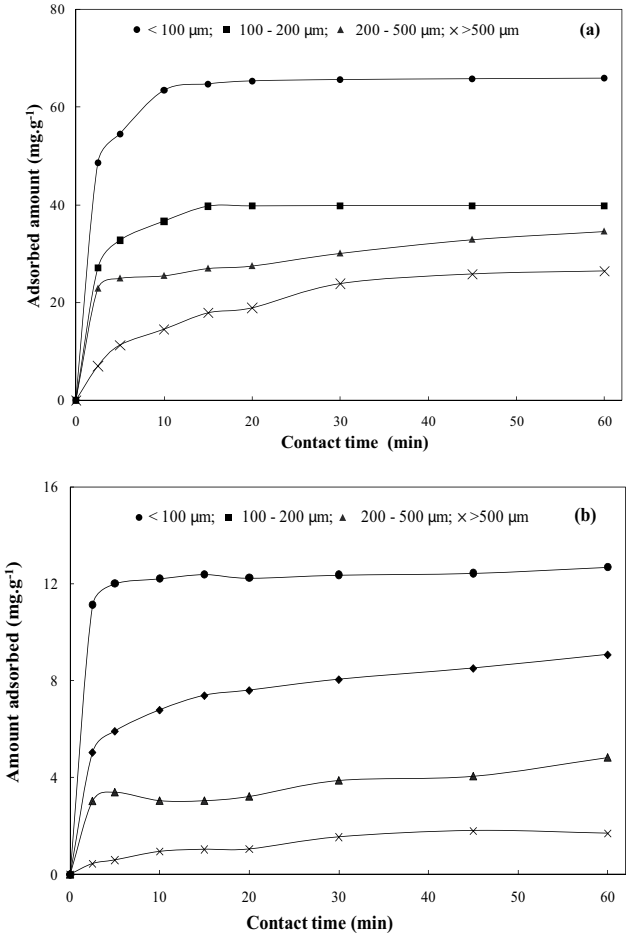

Fig. 8. Effect of CCS particle size on MB and CR adsorption. Operating conditions: C_0 = 500 mg L^{-1}, dose of CCS = 7.5 g L^{-1} (MB) and 20 g L^{-1} (CR), volume of solution = 200 mL, agitation speed = 200 rpm and T = 25°C.

3.3. Effect of the composition of the dye mixture

Effect of the composition of the dye mixture on the adsorption capacity of CCS is investigated using different dye mass ratios. Results presented in Fig. 9 show that in the case of a single dye adsorption onto CCS, MB dye (q_e = 66.28 mg g^{-1}) is better adsorbed than CR (q_e = 18 mg g^{-1}). However, in the binary system (MB + CR), the adsorbed amount of CR increases from 3.9 to 38.62 mg g^{-1} with the increase of CR concentration in the binary mixture, remaining almost constant for MB (24.9 mg g^{-1}). The adsorption of MB and CR in the binary mixture seems to be selective.

Thus, saturation of CCS is achieved for the cationic dye (MB) for different compositions, leading to an increase in the adsorbed amount of anionic dye (CR) by decreasing its mass ratio in the binary mixture. This could be due to an increase in the interactions between CR molecules, increasing its concentration and reducing adsorption ability.

3.4. Kinetic study of the adsorption process

The influence of contact time on the adsorption of MB and CR is analysed. Adsorption experiments were conducted at different time intervals, keeping the volume of contact (V = 200 mL) constant, the initial dye concentration (C_0 = 500 mg L^{-1}) at room temperature and applying a dose of CCS of 7.5 g L^{-1} for MB and 20 g L^{-1} for CR and MB–CR. Figs. 10a–c display UV–Vis spectra for aqueous solutions of MB, CR and MB–CR at different contact times with CCS. It should be noted that a rapid decrease in the absorbance within the first 5 min takes place, indicating a fast adsorption towards both anionic and cationic dyes. A clean surface of CCS facilitates a fast adsorption and makes the co-adsorption of MB–CR aggregates possible.

After 5 min of adsorption time, the absorbance of MB and CR decreases to 82% and 61.5% for single adsorption, and 99.5% and 99% for co-adsorption, respectively. The insets

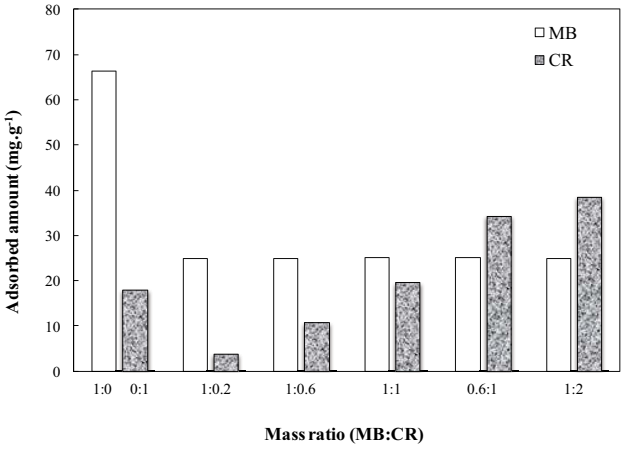

Fig. 9. Effect of varying the initial composition of a mixture of dyes (MB and CR) on the adsorption capacity of CCS. Operating conditions: dose of CCS = 20 g L^{-1}, C_0 = 500 mg L^{-1} for MB and 100–1,000 mg L^{-1} for CR, contact time = 24 h, agitation speed = 200 rpm and T = 25°C.

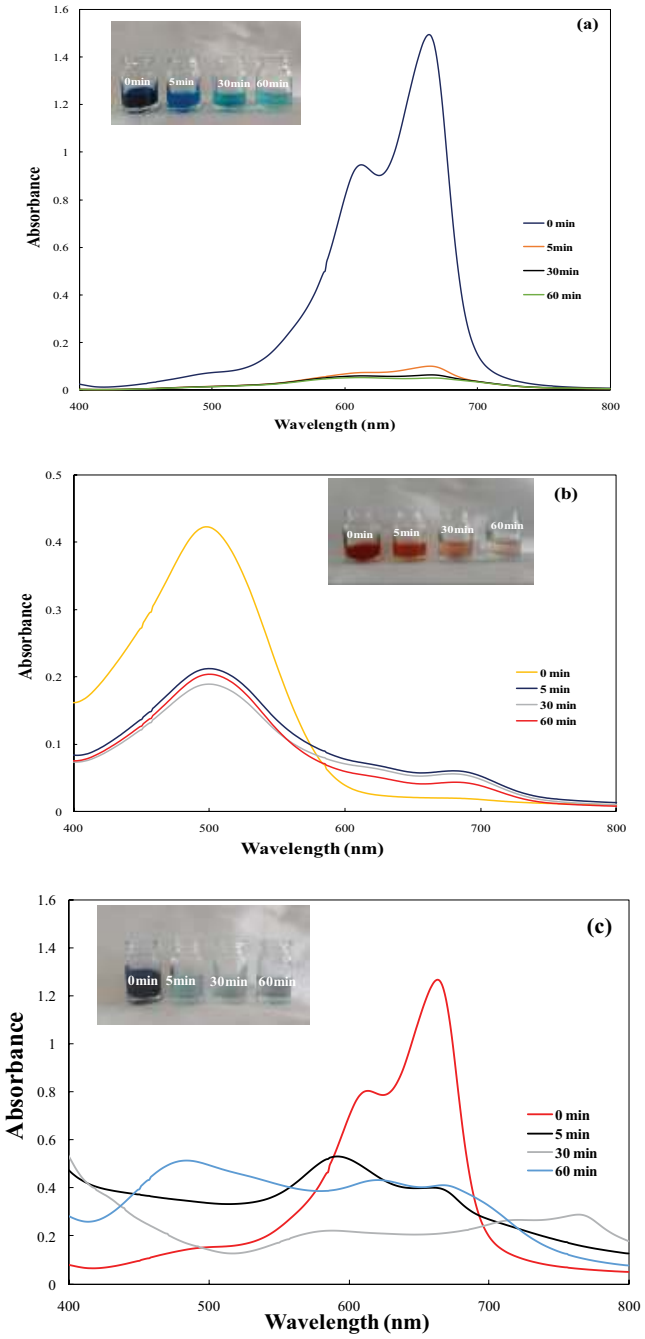

Fig. 10. Variation of UV–Vis absorbance spectra as a function of time for MB (a), CR (b), and a mixture of MB–CR (c) during the adsorption onto CCS. Operating conditions: C_0 = 500 mg L^{-1}, dose of CCS = 7.5 g L^{-1} (MB) and 20 g L^{-1} (CR and MB–CR), contact time = 24 h, agitation speed = 200 rpm and T = 25°C. Each sample was diluted (50 times for MB, 25 times for CR and MB–CR) before UV–Vis measurements.

in Fig. 10 visually demonstrate the colour changes of the samples after the adsorption of dyes onto CCS.

Curves displayed in Fig. 11 indicate that the adsorption capacity of CCS for both dyes in single and binary mixture increases rapidly with the contact time in the first stage of the adsorption process. After that, the adsorption rate gradually

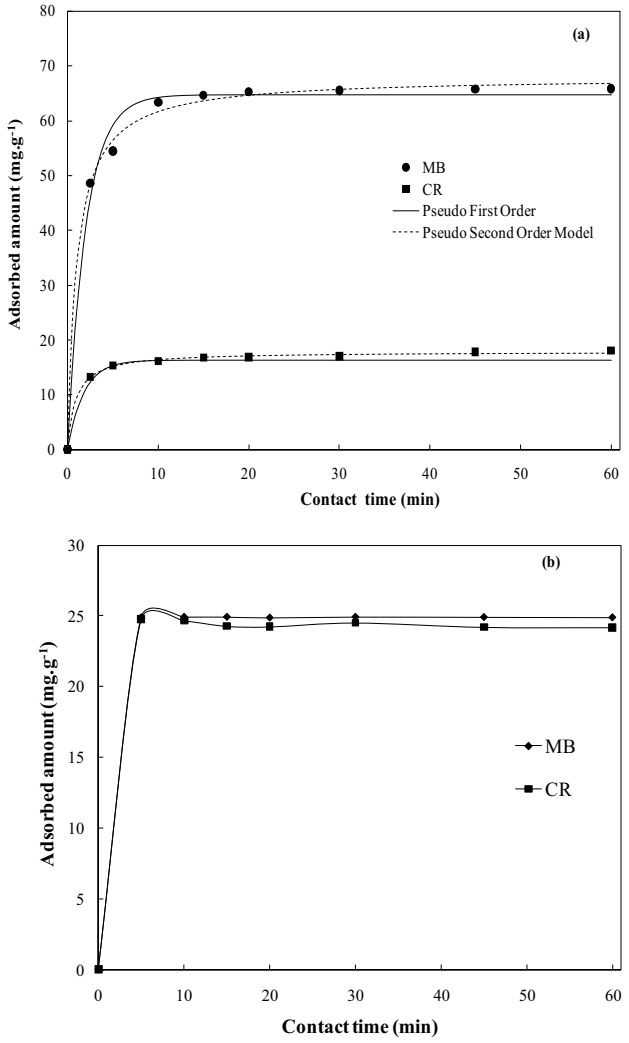

Fig. 11. Effect of contact time on the adsorption capacity of CCS towards MB and CR in single (a) and binary mixture of dyes (b). Operating conditions: C_0 = 500 mg L^{-1}, dose of CCS = 7.5 g L^{-1} (MB) and 20 g L^{-1} (CR and MB–CR), agitation speed = 200 rpm and T = 25°C.

becomes slow and reaches equilibrium values at 30, 20, 15 and 5 min for MB, CR in the single system and in the binary mixture, respectively. The adsorbed amount for MB and CR is equal to 65.85 and 18.11 mg g^{-1} in the single system; and 24.87 and 24.18 mg g^{-1} in the binary mixture, respectively.

These results are attributed to the fact that at the initial stage of the adsorption process the number of vacant adsorption sites available for the adsorption of dye molecules is high. With an increase of the contact time of the adsorption process, the number of adsorption sites accessible to interact with the residual dye molecules decrease [17].

In order to assess the adsorption kinetics of the studied dyes onto CCS, pseudo-first-order and pseudo-second-order kinetic models are fitted to the experimental data:

The pseudo-first-order kinetic model [18] is given by:

$$q_t = q_e\left(1 - e^{-k_1 t}\right) \quad (5)$$

where q_t and q_e are the adsorption capacities at time t and at equilibrium time, respectively; and k_1 is the pseudo-first-order model rate constant.

The pseudo-second-order kinetic model reported by Ho et al. [19] is represented as:

$$q_t = \frac{k_2 q_e^2 t}{1 + k_2 q_e t} \tag{6}$$

where k_2 is the adsorption rate constant.

Both non-linear models were fitted to the experimental data using OriginPro 8 software. Parameter values are given in Table 2. The model fitting was evaluated from the determination coefficient (R^2), the adjusted determination coefficient (R^2_{adj}), reduced chi-square and standard deviation (SD) of residues [20]. The difference between the theoretical and experimental quantities of dyes adsorbed by CCS was measured using SD. The best fit model is the one with the lowest value of SD and the one in which the value of R^2_{adj} is closer to unity. Eqs. (7)–(10) depict the expressions of reduced Chi-square, standard deviation (SD), determination coefficient (R^2) and adjusted determination coefficient (R^2_{adj}), respectively.

$$\text{Reduced Chi} - \text{Squared} = \sum_i^n \frac{\left(q_{i,\text{exp}} - q_{i,\text{model}}\right)^2}{n-p} \tag{7}$$

$$\text{SD} = \sqrt{\left(\frac{1}{n-p}\right) \times \sum_i^n \left(q_{i,\text{exp}} - q_{i,\text{model}}\right)^2} \tag{8}$$

$$R^2 = \left[\frac{\sum_i^n \left(q_{i,\text{exp}} - \bar{q}_{\text{exp}}\right)^2 - \sum_i^n \left(q_{i,\text{exp}} - q_{i,\text{model}}\right)^2}{\sum_i^n \left(q_{i,\text{exp}} - \bar{q}_{\text{exp}}\right)^2} \right] \tag{9}$$

$$R^2_{\text{adj}} = 1 - \left(1 - R^2\right) \times \left(\frac{n-1}{n-p-1}\right) \tag{10}$$

where $q_{i,\text{model}}$ is each value of q predicted by the fitted model, $q_{i,\text{exp}}$ is each value of q measured experimentally, $\bar{q}_{\text{exp}}$ is the average of q experimentally measured, n is the number of experiments and p is the number of parameters in the model.

The obtained data presented in Table 2 shows that the calculated values for the adsorption capacities (q_e) agreed well with experimental values (q_{exp}) and confirm that the pseudo-second-order kinetic model is the most suitable model for describing MB and CR adsorption kinetics on CCS with the highest correlation coefficient (R^2 = 0.99), adjusted determination coefficient (R^2_{adj}) and low standard deviation (SD).

3.5. Adsorption isotherms

The adsorption isotherm indicates how the adsorbate molecules are distributed between the liquid and solid phases when the adsorption process reaches the equilibrium [21]. The analysis of the equilibrium data fit to different isotherm models is an important step in determining the most suitable model.

Fig. 12 represents the total amount of adsorbed dyes onto CCS at the equilibrium (q_e). The Langmuir, Freundlich and Dubinin–Radushkevich isotherm models were fitted to the experimental equilibrium data. Mathematical expressions of such models are presented in Eqs. (11)–(14), respectively [22–24]. Table 3 summarises calculated parameters, SD and correlation coefficients for each adsorption isotherm model, estimated by a non-linear regressive method.

$$q_e = \frac{q_m K_L C_e}{1 + K_L C_e} \tag{11}$$

$$q_e = K_F C_e^{1/n} \tag{12}$$

Table 2
Kinetic model parameters of the adsorption of MB and CR dyes onto CCS

Kinetic model	Parameters	MB	CR
Pseudo-first-order	q_{exp} (mg g^{-1})	65.85	18.11
	q_e (mg g^{-1})	64.79	17.07
	k_1 (min^{-1})	0.49	0.56
	R^2	0.90	0.98
	R^2_{adj}	0.98	0.98
	Reduced Chi-sqr (mg g^{-1})	4.89	0.45
	SD (mg g^{-1})	0.90	0.27
Pseudo-second-order	q_{exp} (mg g^{-1})	65.85	18.11
	q_e (mg g^{-1})	68	17.87
	k_2 (g mg^{-1} min^{-1})	0.014	0.063
	R^2	0.99	0.99
	R^2_{adj}	0.99	0.99
	Reduced Chi-sqr (mg g^{-1})	1.42	0.09
	SD (mg g^{-1})	0.65	0.16

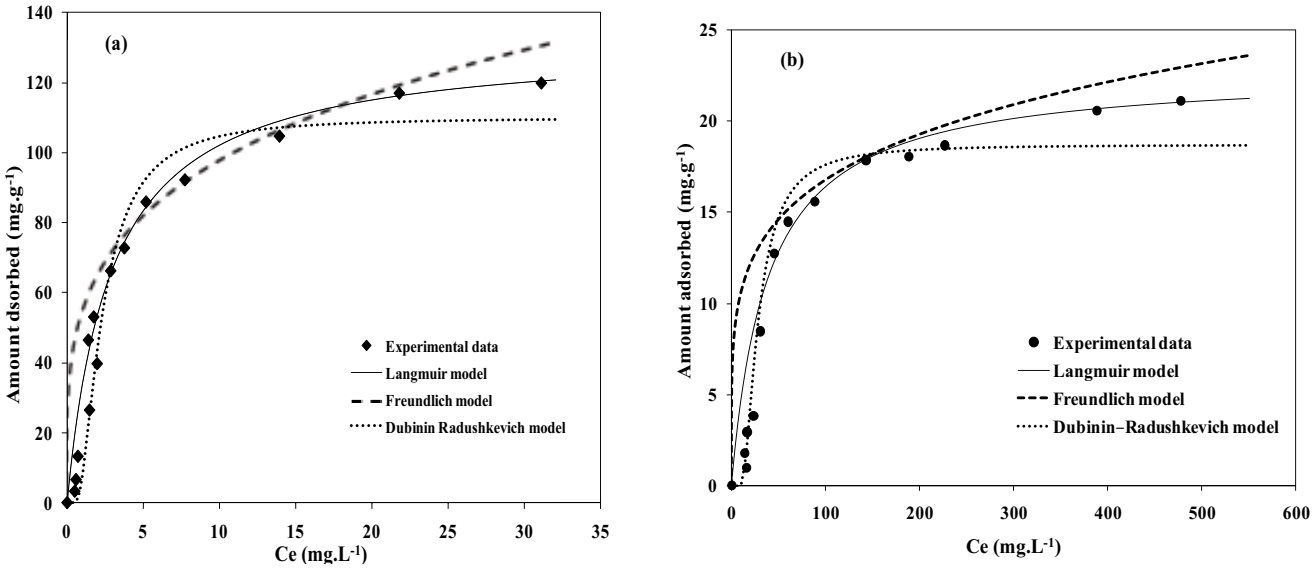

Fig. 12. Adsorption equilibrium data of MB and CR onto CCS: (a) MB and (b) CR. Operating conditions: contact time = 1 h, dose of CCS = 7.5 g L^{-1} (MB) and 20 g L^{-1} (CR), agitation speed = 200 rpm and T = 25°C.

Table 3
Isotherm constant parameters and correlation coefficients calculated for the adsorption of MB and CR onto CCS

Models	Parameters	MB	CR
Langmuir	q_m (mg g^{-1})	144	25.02
	K_L (L mg^{-1})	0.23	0.014
	R^2	0.98	0.98
	R^2_{adj}	0.946	0.94
	Reduced Chi-sqr (mg g^{-1})	97.47	4.13
	SD (mg g^{-1})	9.75	1.65
Freundlich	K_F (mg g^{-1}) (L $mg^{-1})^{1/n}$	33.71	2.14
	n	2.40	2.59
	R^2	0.96	0.95
	R^2_{adj}	0.87	0.84
	Reduced Chi-sqr (mg g^{-1})	233.20	10.67
	SD (mg g^{-1})	4.65	0.72
Dubinin–Radushkevich	q_m (mg g^{-1})	109.58	19.69
	B (mol^2 J^{-2})	7.67×10^{-7}	1.44×10^{-4}
	R^2	0.93	0.96
	R^2_{adj}	0.93	0.97
	Reduced Chi-sqr (mg g^{-1})	121	1.97
	SD (mg g^{-1})	5.21	0.55

$$q_e = q_m \exp\left(-B\,\varepsilon^2\right) \tag{13}$$

$$\varepsilon = RT \ln\left(1 + \frac{1}{C_e}\right) \tag{14}$$

where K_L (L mg^{-1}) is the Langmuir equilibrium constant, q_m and q_e (mg g^{-1}) are the Langmuir maximum and equilibrium adsorption capacity, respectively. C_e is the equilibrium concentration of the adsorbate (mg L^{-1}). K_F ((mg g^{-1}) (L $mg^{-1})^{1/n}$) is the Freundlich constant and $1/n$ is the heterogeneity factor. B (mol^2 J^{-2}) is a constant related to the adsorption energy, ε represents the Polanyi potential, R is the gas constant (8.314 J mol^{-1} K^{-1}) and T is the temperature (K).

The constant B estimates the mean free energy of adsorption (E, kJ mol^{-1}), which is calculated by the following equation:

$$E = \frac{1}{\sqrt{2B}} \tag{15}$$

The magnitude of adsorption energy is used to estimate the adsorption mechanism as chemical (E = 8–16 kJ mol^{-1}), or physical adsorption (E < 8 kJ mol^{-1}). The mean adsorption energy (E) obtained for MB and CR adsorption were 2.23 and 0.74 kJ mol^{-1}, respectively; indicating that a physical adsorption mechanism takes place.

The dimensionless constant of Langmuir isotherm model (equilibrium parameter R_L) for the adsorption process of MB and CR dye was calculated from Eq. (16):

$$R_L = \frac{1}{\left(1 + K_L C_0\right)} \tag{16}$$

where K_L and C_0 are the Langmuir adsorption constant (L mg^{-1}) and the initial dye concentration (mg L^{-1}), respectively.

All the calculated R_L values are higher than zero and lower than unity ($0 < R_L < 1$), which reflects a favourable adsorption of MB and CR using CCS.

The obtained results show that CCS has a high affinity towards MB and CR. The tested CCS adsorbent is effective in removing dye at low equilibrium concentrations and reaches the maximum adsorption capacity at the highest concentrations. It is observed that the removal efficiency varied, depending on the type of dye. CCS performed well for the adsorption of lower-molecular weight MB (144 mg g^{-1}) compared with higher molecular weight CR (25.02 mg g^{-1}). The changes in the removal efficiency towards the adsorption of MB and CR onto CCS could be due to several factors that include molecular weight, molecule size, charge and chemical structure, as well as the properties of the adsorbent. Due to the higher negative charge present on the CCS surface, the adsorbent exhibits a greater affinity and adsorptive capacity for MB. At the same time, stronger repulsion appears among the negative charge CCS and CR molecules due to their negative charges, leading to lower adsorption capacity of CR onto the CCS.

The results listed in Table 3 indicate that the best fit of experimental data is obtained with the Langmuir model in comparison with Freundlich and Dubinin–Radushkevich models. The maximum monolayer adsorption capacities are 144 and 25.02 mg g^{-1} for MB and CR, respectively.

In order to show the advantages in the application of CCS as a natural adsorbent for the removal of dyes from contaminated waters, the maximum adsorption capacities of MB and CR onto CCS are compared with previous reported data of various low-cost adsorbents [25–41] (Table 4). As can be observed, the maximum adsorption capacities of MB and CR onto CCS are significantly larger than those reported values in the literature for rice husk, raw date pits, cellulose fibre, cashew net shell, activated carbon, coir pith, carbonised

Table 4
Maximum adsorption capacities of different adsorbents used for the removal of MB and CR

Biosorbent	Dyes	q (mg g^{-1})	References
Cupressus sempervirens	MB	144	This study
	CR	25.02	This study
Rice husk	MB	40.59	[25]
Raw date pits	MB	80.30	[26]
Defatted algal biomass	MB	7.73	[27]
Sugar extracted spent rice biomass	MB	8.13	[28]
Biochar generated from sludge and tea waste	MB	12.58	[29]
Carbonised peanut shell (CPS)	MB	5.34	[30]
Carbonised chestnut (CSS)	MB	5.13	[31]
Sumac leaves	MB	5.80	[32]
Thiourea-modified sugarcane bagasse cellulose	MB	632.90	[33]
Carbonylated cellulose/microfibrillated cellulose spheres (MCMFCs)	MB	303	[34]
Banana stalk waste	MB	243.90	[35]
Palm kernel fibre	MB	217.95	[36]
Sugarcane bagasse	CR	39.80	[37]
Date stones	CR	45.08	[37]
Jujube shells	CR	59.55	[38]
Modified wheat straw	CR	71.20	[39]
Cellulose fibre	CR	17.39	[40]
Eucalyptus wood sawdust	CR	31.25	[41]
Cashew net shell	CR	5.18	[42]
Activated carbon (LT)	CR	1.88	[43]
Coir pith	CR	6.70	[44]
Kaolin	CR	5.44	[45]
Cone pine	CR	40.19	[46]
Saw dust	CR	5.10	[41]

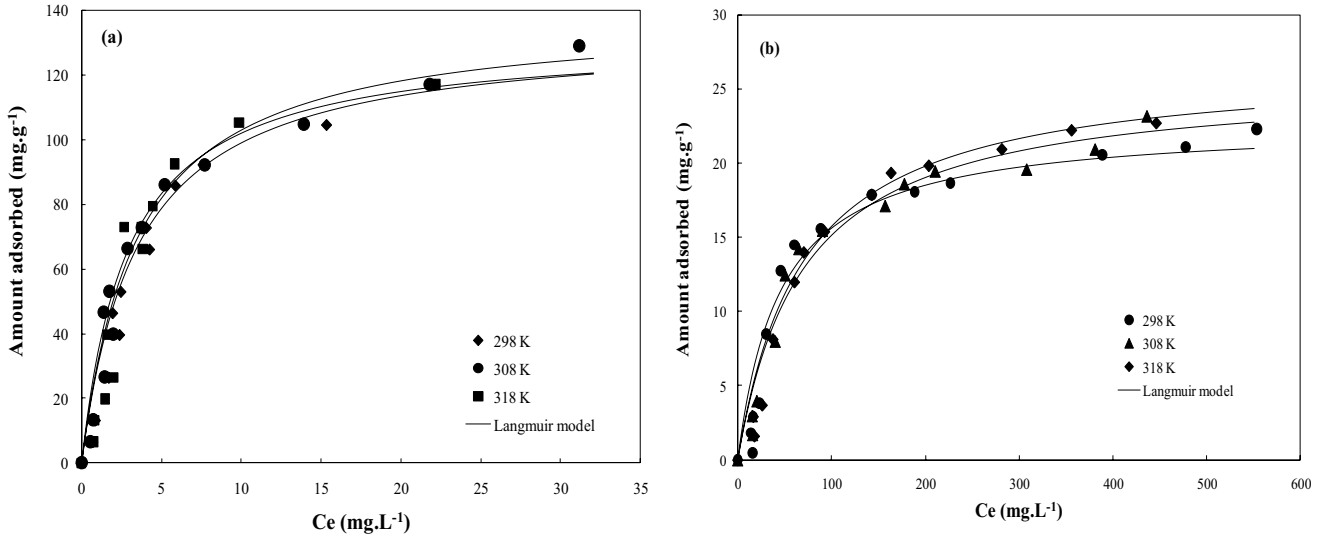

Fig. 13. Effect of temperature on the adsorption of MB and CR onto CCS: (a) MB and (b) CR. Operating conditions: C_0 = 0–1,000 mg L^{-1} and T = 25°C, 35°C and 45°C.

peanut shell (CPS), carbonised chestnut (CSS), sumac leaves and kaolin. However, they are lower than the values reported for banana stalk waste, modified wheat straw, palm kernel fibre, sugarcane bagasse, date stones, thiourea-modified sugarcane bagasse cellulose, carbonylated cellulose/microfibrillated cellulose spheres (MCMFCs) and jujube shells. Such evidences support the statement of the feasibility to employ CCS as natural adsorbent for MB and CR removal from aqueous solutions.

Fig. 13 depicts the effect of temperature on the adsorption of MB and CR onto CCS in the ranging between 25°C and 45°C. As it is shown in Fig. 13, the adsorption capacity of CCS shows a slight increase when temperature rises (from 144 to 150 mg g^{-1} for MB and 25.02 to 28.66 mg g^{-1} for CR). These results could be attributed to an increase on the solubility of dye molecules with the raise in temperature, increasing intraparticle diffusion of MB and CR molecules that leads a higher access to active sites available for dye adsorption.

4. Conclusions

Experimental results confirm that cone powder from Moroccan cypress *Cupressus sempervirens* can be used as a low-cost natural adsorbent for the removal of dyes from aqueous solutions. CCS exhibits a high adsorptive capacity towards MB and CR dye molecules. Infrared studies reveal that dye molecules interact with O–H groups, forming surface complexes via hydrogen bonding. Obtained data reveal a better performance of CCS in removal of MB than CR. A pseudo-second-order kinetic model describes the adsorption process of MB and CR as function of time very well. Maximum adsorption capacities of 144 and 25.02 mg g^{-1} towards MB and CR are obtained, respectively. CCS presents a great potential to be used as an inexpensive and easily available alternative biomass for the removal of dyes from aqueous solutions.

Acknowledgements

The authors are grateful for the financial support provided by the Moroccan Environment Ministry (Project DE-LIX). They would also like to acknowledge the University of Minho for co-financing this research as part of the Erasmus mobility of PhD student Z. Bencheqroun (Erasmus Scholarship) by the projects BioTecNorte (operation NORTE-01-0145-FEDER-000004), PTDC/AAGTEC/5269/2014 and Centre of Chemistry (UID/QUI/00686/2013 and UID/QUI/0686/2016).

References

[1] D. Pokhrel, T. Viraraghavan, Treatment of pulp and paper mill wastewater—a review, Sci. Total Environ., 333 (2004) 37–58.
[2] C. O'Neill, F.R. Hawkes, D.L. Hawkes, N.D. Lourenco, H.M. Pinheiro, W. Delée, Colour in textile effluents - sources, measurement, discharge consents and simulation: a review, J. Chem. Technol. Biotechnol., 74 (1999) 1009–1018.
[3] A.K. Jain, V.K. Gupta, A. Bhatnagar, Suhas, Utilization of industrial waste products as adsorbents for the removal of dyes, J. Hazard. Mater., 101 (2003) 31–42.
[4] Y.S. Ho, G. McKay, Sorption of dyes and copper ions onto biosorbents, Process Biochem., 38 (2003) 1047–1061.
[5] R. Elmoubarki, F.Z. Mahjoubi, H. Tounsadi, J. Moustadraf, M. Abdennouri, A. Zouhri, A. El Albani, N. Barka, Adsorption of textile dyes on raw and decanted Moroccan clays: kinetics, equilibrium and thermodynamics, Water Resour. Ind., 9 (2015) 16–29.
[6] H.P. Boehm, Some aspects of the surface chemistry of carbon blacks and other carbons, Carbon, 32 (1994) 759–764.
[7] W. Stumm, J.J. Morgan, Aquatic Chemistry, 2nd ed., John Wiley and Sons, New York, 1981.
[8] L. Liu, Z.Y. Gao, X.P. Su, X. Chen, L. Jiang, J.M. Yao, Adsorption removal of dyes from single and binary solutions using a cellulose-based bioadsorbent, ACS Sustainable Chem. Eng., 3 (2015) 432–442.
[9] S.J. Allen, G. McKay, J.F. Porter, Adsorption isotherm models for basic dye adsorption by peat in single and binary component systems, J. Colloid Interface Sci., 280 (2004) 322–333.
[10] M.R.H. Mas Haris, K. Sathasivam, The removal of methyl red from aqueous solutions using banana pseudostem fibers, Am. J. Appl. Sci., 6 (2009) 1690–1700.

[11] Z. Belala, M. Jeguirim, M. Belhachemi, F. Addoun, G. Trouvé, Biosorption of basic dye from aqueous solutions by date stones and palm-trees waste: kinetic, equilibrium and thermodynamic studies, Desalination, 271 (2011) 80–87.
[12] M. Danish, R. Hashim, M.N.M. Ibrahim, O. Sulaiman, Optimized preparation for large surface area activated carbon from date (*Phoenix dactylifera* L.) stone biomass, Biomass Bioenergy, 61 (2014) 167–178.
[13] L. Borah, M. Goswami, P. Phukan, Adsorption of Methylene Blue and eosin yellow using porous carbon prepared from tea waste: adsorption equilibrium, kinetics and thermodynamics study, J. Environ. Chem. Eng., 3 (2015) 1018–1028.
[14] A. Gupta, C. Balomajumder, Simultaneous adsorption of Cr(VI) and phenol onto tea waste biomass from binary mixture: multicomponent adsorption, thermodynamic and kinetic study, J. Environ. Chem. Eng., 3 (2015) 785–796.
[15] M. Hadri, Z. Chaouki, K. Draoui, M. Nawdali, A. Barhoun, H. Valdés, N. Drouiche, H. Zaitan, Adsorption of a cationic dye from aqueous solution using low-cost Moroccan diatomite: adsorption equilibrium, kinetic and thermodynamic studies, Desal. Wat. Treat., 75 (2017) 213–224.
[16] M.C. Ncibi, B. Mahjoub, M. Seffen, Kinetic and equilibrium studies of methylene blue biosorption by *Posidonia oceanica* (L.) fibres, J. Hazard. Mater., 139 (2007) 280–285.
[17] P.D. Saha, S. Chakraborty, S. Chowdhury, Batch and continuous (fixed-bed column) biosorption of crystal violet by Artocarpus heterophyllus (jackfruit) leaf powder, Colloids Surf., B, 92 (2012) 262–270.
[18] S. Lagergren, Zur Theorie der Sogenannten Adsorption Gelöster Stoffe, Kungliga Svenska Vetenskapsakademiens, Handlingar, 24 (1898) 1–39.
[19] Y.S. Ho, G. McKay, D.A.J. Wase, C.F. Forster, Study of the sorption of divalent metal ions on to peat, Adsorpt. Sci. Technol., 18 (2000) 639–650.
[20] E.C. Lima, M.A. Adebayo, F.M. Machado, Kinetic and Equilibrium Models of adsorption, Chapter 3, C.P. Bergmann, F.M. Machado, Eds., Carbon Nanomaterials as Adsorbents for Environmental and Biological Applications, Springer International Publishing, Switzerland, 2015, pp. 33–69.
[21] J. Fu, Z. Chen, M. Wang, S. Liu, J. Zhang, J. Zhang, R. Han, Q. Xu, Adsorption of methylene blue by a high-efficiency adsorbent (polydopamine microspheres): kinetics, isotherm, thermodynamics and mechanism analysis, Chem. Eng. J., 259 (2015) 53–61.
[22] I. Langmuir, The adsorption of gases on plane surfaces of glass, mica and platinum, J. Am. Chem. Soc., 40 (1918) 1361–1403.
[23] H.M.F. Freundlich, Over the adsorption in solution, Z. Phys. Chem., 57 (1906) 385–470.
[24] M.M. Dubinin, L.V. Radushkevich, The Equation of the Characteristic Curve of Activated Charcoal, Proceedings of the Academy of Sciences, Physical Chemistry Section, 55 (1947) 331–337.
[25] V. Vadivelan, K.V. Kumar, Equilibrium, kinetics, mechanism, and process design for the sorption of methylene blue onto rice husk, J. Colloid Interface Sci., 286 (2005) 90–100.
[26] F. Banat, S. Al-Asheh, L. Al-Makhadmeh, Evaluation of the use of raw and activated date pits as potential adsorbents for dye containing waters, Process Biochem., 39 (2003) 193–202.
[27] T.S. Chandra, S.N. Mudliar, S. Vidyashankar, S. Mukherji, R. Sarada, K. Krishnamurthi, V.S. Chauhan, Defatted algal biomass as a non-conventional low-cost adsorbent: surface characterization and methylene blue adsorption characteristics, Bioresour. Technol., 184 (2015) 395–404.
[28] M.S.U. Rehman, I. Kim, J.-I. Han, Adsorption of methylene blue dye from aqueous solution by sugar extracted spent rice biomass, Carbohydr. Polym., 90 (2012) 1314–1322.
[29] S. Fan, J. Tang, Y. Wang, H. Li, H. Zhang, J. Tang, Z. Wang, X. Li, Biochar prepared from co-pyrolysis of municipal sewage sludge and tea waste for the adsorption of methylene blue from aqueous solutions: kinetics, isotherm, thermodynamic and mechanism, J. Mol. Liq., 220 (2016) 432–441.
[30] J. Gülen, F. Zorbay, Methylene blue adsorption on a low cost adsorbent-carbonized peanut shell, Water Environ. Res., 89 (2017) 805–816.
[31] J. Gülen, M. İskeçeli, Removal of methylene blue by using porous carbon adsorbent prepared from carbonized chestnut shell, Mater. Test., 59 (2017) 188–194.
[32] J. Gülen, B. Akın, M. Özgür, Ultrasonic-assisted adsorption of methylene blue on sumac leaves, Desal. Wat. Treat., 57 (2016) 9286–9295.
[33] Y. Pan, X. Shi, P. Cai, T. Guo, Z. Tong, H. Xiao, Dye removal from single and binary systems using gel-like bioadsorbent based on functional-modified cellulose, Cellulose, 25 (2018) 2559–2575.
[34] Y. Li, H. Xiao, Y. Pan, L. Wang, Novel composite adsorbent consisting of dissolved cellulose fiber/microfibrillated cellulose for dye removal from aqueous solution, ACS Sustainable Chem. Eng., 6 (2018) 6994–7002.
[35] B.H. Hameed, D.K. Mahmoud, A.L. Ahmad, Sorption equilibrium and kinetics of basic dye from aqueous solution using banana stalk waste, J. Hazard. Mater., 158 (2008) 499–506.
[36] A.E. Ofomaja, Sorption dynamics and isotherm studies of methylene blue uptake on to palm kernel fibre, Chem. Eng. J., 126 (2007) 35–43.
[37] Z.Y. Zhang, L. Moghaddam, I.M. O'Hara, W.O.S. Doherty, Congo red adsorption by ball-milled sugarcane bagasse, Chem. Eng. J., 17 (2011) 122–128.
[38] N. El Messaoudi, A. Dbik, M. El Khomri, A. Sabour, S. Bentahar, A. Lacherai, Date stones of Phoenix dactylifera and jujube shells of Ziziphus lotus as potential biosorbents for anionic dye removal, Int. J. Phytorem., 19 (2017) 1047–1052.
[39] R. Zhang, J. Zhang, X. Zhang, C. Dou, R. Han, Adsorption of Congo red from aqueous solutions using cationic surfactant modified wheat straw in batch mode: kinetic and equilibrium study, J. Taiwan Inst. Chem. Eng., 45 (2014) 2578–2583.
[40] V.K. Gupta, D. Pathania, S. Agarwal, S. Sharma, Amputation of Congo red dye from waste water using microwave induced grafted *Luffa cylindrica* cellulosic fiber, Carbohydr. Polym., 111 (2004) 556–566.
[41] V.S. Mane, B.P.V. Vijay, Kinetic and equilibrium studies on the removal of Congo red from aqueous solution using Eucalyptus wood (*Eucalyptus globulus*) saw dust, J. Taiwan Inst. Chem. Eng., 44 (2013) 81–88.
[42] P. Senthil Kumar, S. Ramalingam, C. Senthamarai, M. Niranjanaa, P. Vijayalakshmi, S. Sivanesan, Adsorption of dye from aqueous solution by cashew nut shell: studies on equilibrium isotherm, kinetics and thermodynamics of interactions, Desalination, 261 (2010) 52–60.
[43] A. Aygün, S. Yenisoy-Karakaş, I. Duman, Production of granular activated carbon from fruit stones and nutshells and evaluation of their physical, chemical and adsorption properties, Microporous Mesoporous Mater., 66 (2003) 189–195.
[44] C. Namasivayam, D. Kavitha, Removal of Congo red from water by adsorption onto activated carbon prepared from coir pith, an agricultural solid waste, Dyes Pigm., 54 (2002) 47–58.
[45] V.K. Gupta, A. Mittal, V. Gajbe, J. Mittal, Adsorption of basic fuchsin using waste materials—bottom ash and deoiled soya—as adsorbents, J. Colloid Interface Sci., 319 (2008) 30–39.
[46] S. Dawood, T.K. Sen, Removal of anionic dye Congo red from aqueous solution by raw pine and acid-treated pine cone powder as adsorbent: equilibrium, thermodynamic, kinetics, mechanism and process design, Water Res., 46 (2012) 1933–1946.